Improved pEKEx2-derived expression vectors for tightly controlled production of recombinant proteins in *Corynebacterium glutamicum*

Patrick J. Bakkes[a], Paul Ramp[a], Astrid Bida[a], Doris Dohmen-Olma[a], Michael Bott[a] and Roland Freudl[a].*

[a] Institute of Bio- and Geosciences, IBG-1: Biotechnology, Forschungszentrum Jülich GmbH, 52425 Jülich, Germany

Address correspondence to P.J. Bakkes, p.bakkes@fz-juelich.de, or R. Freudl, r.freudl@fz-juelich.de.

* Corresponding author: p.bakkes@fz-juelich.de

Abstract

The *Escherichia coli/Corynebacterium glutamicum* shuttle vector pEKEx2 is an IPTG-inducible expression vector that has been used successfully for the synthesis of numerous proteins in *C. glutamicum*. We discovered that the leaky gene expression observed for pEKEx2-derived plasmids relates to reduced functionality of the plasmid-encoded repressor LacI carrying a modified C-terminus, while duplicate DNA sequences in the pEKEx2 backbone contribute to plasmid instability. We constructed the pEKEx2-derivatives pPBEx2 and pPREx2, which harbor a restored *lacI* gene and which lack the unnecessary duplicate DNA sequences. pPREx2 in addition enables fusion of target genes to a C-terminal Strep-tag II coding region for easy protein detection and purification. In the absence of inducer, the novel vectors exhibit tight gene repression in *C. glutamicum*, as shown for the secretory production of *Fusarium solani pisi* cutinase and the cytosolic production of green fluorescent protein and *C. glutamicum myo*-inositol dehydrogenase. Undesired heterogeneity amongst clones expressing cutinase from pEKEx2 was attributed to the loss of a vector fragment containing the cutinase gene, which likely occurred via homologous recombination of the identical flanking DNA sequences. Such loss was not observed for pPBEx2. Using pPREx2, IolG-Strep was successfully produced and purified to homogeneity by Strep-Tactin affinity chromatography, obtaining 1.5 mg IolG with a specific activity of 27 µmol·min^{-1}·(mg protein)$^{-1}$ from 100 mL culture. The tight gene repression in the absence of inducer and the improved plasmid stability make expression vectors pPBEx2/pPREx2 attractive alternatives to the available molecular tools for genetic manipulation and high-level production of recombinant proteins in *C. glutamicum.*

Keywords: *Corynebacterium glutamicum,* gene repression, IPTG-inducible expression, protein production, affinity tag, plasmid stability.

Highlights

- Leaky gene expression from pEKEx2 plasmids is due to reduced functionality of an altered plasmid-encoded repressor LacI.
- Duplicate DNA sequences in the pEKEx2 backbone contribute to plasmid instability.
- Novel pEKEx2-based vectors, harboring a restored *lacI* gene and lacking the unfavorable duplicate DNA sequences, were created.
- In contrast to pEKEx2, the offspring vectors pPBEx2/pPREx2 exhibit tight control of target gene expression in *C. glutamicum*.
- pPBEx2/pPREx2 enable high-level production of recombinant proteins, with or without an affinity tag, in *C. glutamicum.*

1. Introduction

The Generally Recognized as Safe (GRAS) bacterium *Corynebacterium glutamicum* is a well-established microbial host for the industrial production of amino acids and organic acids that is gaining importance also in the production of recombinant proteins (Freudl, 2017; Lee et al., 2016). To fully exploit the biotechnological potential of *C. glutamicum*, suitable expression systems are instrumental to achieving high-level protein production (Lee and Kim, 2018). Herein, a tight control of gene expression and high-level gene expression under fully induced conditions are much desired properties. Since the early 1990s a variety of different expression vectors have been developed for *C. glutamicum* that are largely based on native corynebacterial plasmids and genetic elements derived from *E. coli*-based expression vectors (Eggeling and Reyes, 2005; Kang et al., 2014; Kortmann et al., 2015; Lee et al., 2016). An important example is the well-established *E. coli*/*C. glutamicum* shuttle vector pEKEx2, which harbors the *C. glutamicum* origin of replication (ori) from pBL1 and the *E. coli* ColE1 replicon (Eikmanns et al., 1991; Eikmanns et al., 1994). To allow for IPTG-inducible gene expression, pEKEx2 contains the *lac* repressor allele *lacI*^{q} and the *tacI* promoter (Amann et al., 1988; de Boer et al., 1983), along with a kanamycin resistance (Kan^{r}) determinant for plasmid selection that is operative in both *C. glutamicum* and *E. coli*.

pEKEx2 was first described in 1994 and was shown to facilitate the expression of the *glt*A gene coding for citrate synthase from *C. glutamicum* (Eikmanns et al., 1994) and shortly after, the complete nucleotide sequence of pEKEx2 was published (GenBank: AY585307.1). Since then, numerous studies have appeared that report on successful protein production in *C. glutamicum* using pEKEx2 (Baumgart et al., 2013; Gauttam et al., 2019; Jurischka et al., 2020) or related plasmids such as the parental pEKEx1 (Eikmanns et al., 1991) and offspring plasmids such as pEKEx3 (Stansen et al., 2005), pAN6 (Frunzke et al., 2008), or pOGOduet (Goldbeck and Seibold, 2018). However, when using pEKEx2-derived plasmids, it is frequently noticed that substantial gene expression occurs already in the absence of the inducer (Goldbeck and Seibold, 2018; Jurischka et al., 2020; Kortmann et al., 2015; Lausberg et al., 2012). In biotechnological and physiological studies, a stringent control of gene expression is typically

preferred and leaky gene expression is usually considered an unwanted property, especially in cases when even minor levels of target gene expression are detrimental to the expression host.

The phenomenon of leaky gene expression generally associated with pEKEx2-based plasmids prompted us to examine the published nucleotide sequence of pEKEx2, which revealed an incorrect DNA coding region for the repressor LacI, which likely contributes to the significant gene expression observed in the absence of inducer (IPTG). In addition, we noticed unfavorable duplicate DNA sequences in the pEKEx2 backbone, which may contribute to plasmid instability. Based on this knowledge, we constructed the pEKEx2-derived expression vectors pPBEx2 and pPREx2, which carry the correct *lacI* DNA coding sequence and which lack the undesired duplicate DNA regions. The expression performance of pPBEx2 and pPREx2 in *C. glutamicum* was investigated by studying the secretory production of a cutinase from the fungus *Fusarium solani pisi*, as well as the cytoplasmic production of GFP and a *myo*-inositol dehydrogenase from *C. glutamicum*. Importantly, we found that, in contrast to pEKEx2, the offspring plasmids pPBEx2 and pPREx2 exhibit tight gene repression in the absence of the inducer IPTG, indicating that full LacI functionality was achieved. Moreover, removal of the undesired duplicate DNA sequences from the pEKEx2 backbone appeared to improve plasmid stability.

2. Material and methods

2.1 Bacterial strains, plasmids and standard cultivation conditions.

The bacterial strains and plasmids used in this work are shown in Table 1. *E. coli* was grown in LB (lysogeny broth) medium (Bertani, 1951) at 37 °C, whereas *C. glutamicum* was cultivated in BHIS medium containing 37 g/L brain heart infusion (BHI, Difco Laboratories) and 91 g/L sorbitol or BHI + 2% (w/v) glucose at 30 °C. For selection of plasmid-containing clones, in all cases kanamycin was added to the medium; 50 µg/mL in case of *E. coli* and 25 µg/mL in case of *C. glutamicum*.

Table 1. Bacterial strains and plasmids.

Bacterial strains and plasmids	Properties	Source/reference
Bacterial strains		
E. coli DH5α	F$^-$ Φ80*lac*ZΔM15 Δ(*lac*ZYA-*arg*F) U169 *rec*A1 *end*A1 *hsd*R17(r_k^-, m_k^+) *pho*A *sup*E44 *thi*-1 *gyr*A96 *rel*A1 λ$^-$	(Thermo Fisher Scientific, Langerwehe, Germany)
E. coli XL1-Blue	*recA1 endA1 gyrA96 thi-1 hsdR17 supE44 relA1 lac* [F´ *proAB lacI*^{q}Z∆*M15* Tn*10* (Tet^r)].	(Agilent, Heidelberg, Germany)
C. glutamicum ATCC13032	Wild-type.	(Kinoshita et al., 1957)
C. glutamicum ATCC13032 K9	*htrA*::*htrA´-eyfp* (replacement of *htrA* by *htrA´-eyfp*); biosensor strain used for secretion experiments.	(Jurischka et al., 2020)
Plasmids		
pEKEx2	*E. coli/C. glutamicum* shuttle vector; P*tacI*; *lacI*^{q}; $ori_{C.g}$ from pBL1.; $ori_{E.c.}$ ColE1 from pUC18; Kan^r.	(Eikmanns et al., 1994)
pEKEx2-NprE-cutinase	pEKEx2 containing a gene encoding the signal peptide from the *B. subtilis* protease NprE fused to the mature part of the cutinase from *F. solani pisi* (Brockmeier et al., 2006). A consensus *rbs* (AAGGAG) for *C. glutamicum* (Pfeifer-Sancar et al., 2013) followed by an 8 nucleotide spacer (ATATAGAT) is located between the *Pst*I site and the ATG start codon of the fusion gene.	(Hemmerich et al., 2019)
pEKEx2-GFP	pEKEx2 containing the *gfp* gene; Kan^r.	(Lausberg et al., 2012)
pAN6	pEKEx2 derivative with modified multiple cloning site including an *Nde*I site and a Strep-tag II-encoding sequence.	(Frunzke et al., 2008)

pCLTON1	*C. glutamicum* expression vector with *B. subtilis* P*tet* and the *tetR* gene under control of *C. glutamicum* constitutive P*gap*; Kan^r.	(Lausberg et al., 2012)
pCLTON1-GFP	pCLTON1 containing the *gfp* gene; Kan^r.	(Lausberg et al., 2012)
pPBEx2	Cured pEKEx2-derivative containing a correct *lacI*^{q} allele and lacking replicate sequences by deletion of nucleotides 930-1140 within the *Dra*I-*Sap*I region. The *Eco*RI site in the MCS was removed by point mutation; Kan^r.	This study
pPBEx2-NprE-cutinase	The *nprE-cutinase* fusion gene from pEKEx2-NprE-cutinase was cloned into pPBEx2 via *Pst*I and *Sac*I; Kan^r.	This study
pPBEx2-GFP	The *gfp* gene was cloned into pPBEx2 via *Pst*I and *Kpn*I; Kan^r.	This study
pPREx2	pPBEx2 derivative (P*tacI*, *lacI*^{q}, $ori_{C.g}$ from pBL1.; $ori_{E.c.}$ ColE1 from pUC18), with a consensus *rbs* (AAGGAG) for *C. glutamicum* (Pfeifer-Sancar et al., 2013) followed by an 8 nucleotide spacer (ATATACAT), and a modified cloning site including *Nde*I and *Eco*RI restriction sites, and a Strep-tag II-encoding sequence; Kan^r	This study
pPREx2-IolG-Strep	pPREx2 derivative for overproduction of IolG with a C-terminal Strep-tag II, cloned via *Nde*I and *Nhe*I; Kan^r	This study

2.2 General molecular biology procedures.

DNA manipulations were carried out according to standard protocols (Green and Sambrook, 2012). FastDigest restriction enzymes and T4 DNA ligase were from Thermo Fisher Scientific (Langerwehe, Germany), while oligonucleotides were purchased from Eurofins (Ebersberg, Germany). PCR conditions were optimized for each primer pair. DNA fragments were amplified by PCR using Phusion DNA polymerase (Thermo Fisher Scientific, Langerwehe, Germany) and purified using the NucleoSpin gel and PCR clean up kit from Macherey-Nagel (Düren, Germany). Recombinant plasmids were isolated from *E. coli* or *C. glutamicum* transformants using the Nucleospin plasmid purification kit from the same manufacturer. DNA sequencing

was carried out by Eurofins (Ebersberg, Germany). For plasmid construction via Gibson DNA assembly (Gibson, 2011), the Gibson Assembly Cloning Kit from New England BioLabs (Frankfurt am Main, Germany) was used. Design of Gibson oligonucleotide pairs and Gibson DNA assembly were carried out according to the manufacturer's recommendations and instructions provided on the NEB website: https://international.neb.com/protocols/2012/12/11/gibson-assembly-protocol-e5510 (last accessed 08/21/2020). DNA concentrations were determined using a NanoDrop spectrophotometer (Thermo Fisher Scientific). Protein concentrations were determined using a BCA assay (Thermo Fisher Scientific) using different concentrations of bovine serum albumin (BSA) as standard.

2.3 Plasmid construction.

2.3.1 Construction of pPBEx2 and derivatives.

Vector **pPBEx2** was constructed via Gibson assembly (Gibson, 2011). For this purpose, four Gibson oligonucleotide pairs (Table 2, G1-4) were designed using appropriate overlapping DNA sequences (Table 2). In addition, to facilitate cloning of the Brockmeier signal peptide library (Brockmeier et al., 2006) into the novel vector for prospective protein secretion studies, the *Eco*RI site in the multiple cloning site (MCS) from pEKEx2 was disrupted by point mutation GAAT[T→***A***]C (Table 2, G1 primer pair). For the construction of pPBEx2, first four separate standard PCR reactions were carried out to amplify the desired Gibson assembly fragments. To generate fragments 1, 2 and 4, pEKEx2 was used as template. For amplification of fragment 1 (0.9 kb), which ranges from the disrupted *Eco*RI site to the ∆930-1140 deletion site, primers G1f and G2r were used for amplification. For amplification of fragment 2, which starts from the ∆930-1140 deletion site and harbors the ColE1 *ori* from pUC18 (*E. coli*), Kan^r and the pBL1 *ori* (*C. glutamicum*), and extends into the corrected coding region for the extreme C-terminus of LacI, the primer pair G2f and G3r was used. For the amplification of this large 5.5 kb fragment, DMSO (3% v/v) was included in the PCR reaction mixture. The correct *lacI* DNA sequence

was amplified from a pTrc99A-derived plasmid (Amann 1988) using primers G3f and G4r, thus yielding fragment 3 (1.1 kb). Finally, primers G4f and G1r were used to generate fragment 4 (0.5 kb), which harbors the *lacI*^{q} promoter region, P*tacI* and the MCS from pEKEx2 (now with disrupted *Eco*RI site). After PCR, template DNA was removed from the reactions by *Dpn*I treatment and the PCR products were purified.

Table 2. Oligonucleotides used for the construction of pPBEx2, pPREx2 and their derivatives**.**

Primer name	Sequence (5'→3')
Gibson assembly	
G1f_ ΔEcoRI	**A**CACTGGCCGTCGTTTTACAGC
G1r_ ΔEcoRI	GCTGTAAAACGACGGCCAGTG**T**ATTCGAGCTCGGTAC
G2f_ Δ930-1140	GCTCTTCCGCTTCCTCGCTCACTGACTCGCTGCGCTCGGTCGTTC
G2r_ Δ930-1140	GAGCGAGGAAGCGGAAGAGCCTATGACATGATTACGAATTAC
G3f_C-LacI	TCACTGCCCGCTTTCCAGTCG
G3r_C-LacI	CGACTGGAAAGCGGGCAGTGAGCGAGGGCGTGCAAGATTC
G4f_N-LacI	ATTCACCACCCTGAATTGACTC
G4r_N-LacI	GAGTCAATTCAGGGTGGTGAATGTGAAACCAGTAACGTTATACGATG
G5f_pPBEx2_ΔNdeI	AGCTACCAACTCA**A**ATGCACGGG
G5r_pPBEx2_ΔNdeI	CCCGTGCAT**T**TGAGTTGGTAGCTC
G6f_up_MCS	CTTCTGGCGTCAGGCAGCCATC
G6r_up_MCS	ATGGCTGCCTGACGCCAGAAG
G7f_down_MCS	ATTCAACATTTCCGTGTCGCCC
G7r_down_MCS	GCGACACGGAAATGTTGAATAC
Standard PCR	
p1f_x2gfp	GCTTGCATGCCTGCAGAAGGAGATATAG
p2r_gfp	TCAGTCTAGGTACCTTATTTGTAGAGCTCATCCATG
p3f_iolG	GCAGAAGGAGATATACATATGAGCAAGAGCCTTC
p4r_iolG	TTACTTCTCGAACTGTGGGTGGGACCAGCTAGCAGCGTAGAAATCTGGGCGAGG

Point mutations disrupting the restriction sites *Eco*RI and *Nde*I of pEKEx2 are shown in bold.

For Gibson assembly, the PCR fragments 1, 2, 3 and 4 were combined at a respective molar ratio of 2:1:2:4, using 100 ng of fragment 2 as vector backbone. Next, chemically competent

E. coli XL1-Blue (100 µL) cells were transformed with 2 µL of the Gibson assembly mix via a standard heat-shock procedure (Cohen et al., 1972). Cells were plated on LB agar plates containing 50 µg/mL kanamycin and incubated overnight at 37 °C. Single colonies were then transferred to liquid LB_{kan} medium (8 mL) and grown overnight at 37 °C and 250 rpm. Recombinant plasmids were isolated from the overnight cultures and analyzed by enzymatic digestion and by DNA sequencing of the entire plasmid, which confirmed that the desired correct DNA sequence for pPBEx2 had been obtained.

For the construction of **pPBEx2-NprE-cutinase,** pEKEx2-NprE-cutinase was digested with *Pst*I and *Sac*I. The *Pst*I-*Sac*I fragment containing the *C. glutamicum* consensus *rbs* and the *nprE-cutinase* fusion gene (Table 1) was gel extracted and ligated into gel purified *Pst*I-*Sac*I-cleaved pPBEx2 vector. In case of **pPBEx2-GFP,** the *gfp* gene from pEKEx2-GFP (Table 1) was amplified, using primers p1f and p2r (Table 2). The respective *gfp* gene encodes the GFPuv variant (GenBank APD28479.1) of the wild-type GFP from the jellyfish *Aequorea victoria*, which has been optimized for maximal fluorescence when excited by UV light (Crameri et al., 1996).

The PCR product was subsequently digested with *Pst*I and *Kpn*I, purified and ligated into gel extracted *Pst*I-*Kpn*I-cleaved pPBEx2 vector. After ligation and transformation of *E. coli* DH5α with the pPBEx2-derived constructs, recombinant plasmids were isolated from different clones and analyzed with appropriate restriction enzymes. DNA sequencing confirmed that the correct DNA sequence had been obtained for both the pPBEx2-NprE-cutinase and the pPBEx2-GFP construct. For expression studies, the plasmids were electroporated into *C. glutamicum* cells as described previously (Eggeling and Bott, 2005) and the recombinant strains were grown on BHIS agar plates containing 25 µg/mL kanamycin.

2.3.2 Construction of pPREx2 and pPREx2-IolG-Strep.

Vector **pPREx2** was constructed by means of Gibson assembly (Gibson, 2011). For this purpose, three Gibson oligonucleotide pairs were designed (Table 2). For the construction of pPREx2 three separate standard PCR reactions were carried out to amplify the desired Gibson

assembly fragments. To generate fragments 1 and 2, pPBEx2 was used as template. Both fragments assemble at the unique *Nde*I site in pPBEx2 and destroy it upon recombination by point mutation CA[T→***A***]ATG (Table 2). For amplification of fragment 1 (~3.5 kb), the primers G5f and G6r were used, while for fragment 2 (~3.6 kb) the primers G7f and G5r were used. Finally, for fragment 3 (~0.9 kb), the primer pair G6f and G7r was used with pAN6 as template to amplify the MCS containing an *Nde*I, *Nhe*I and *Eco*RI site and the Strep-tag II. After PCR, template DNA was removed from the reactions by *Dpn*I treatment and the PCR products were purified.

For Gibson assembly the PCR fragments 1, 2 and 3 were combined at a respective molar ratio of 1:1:2, using 100 ng of fragment 1 as vector backbone. Chemically competent *E. coli* DH5α cells were transformed with 2 µL of the Gibson reaction mix. Recombinant plasmids were isolated from several clones and analyzed with appropriate restriction enzymes. DNA sequencing confirmed that the correct DNA sequence had been obtained. For the construction of **pPREx2-IolG-Strep**, the gene *iolG* (cg0204) was amplified from genomic DNA of *C. glutamicum* using the primer pair p3f and p4r (Table 2). The purified PCR product was cloned into pPREx2 linearized with *Nde*I and *Nhe*I via Gibson assembly. *C. glutamicum* ATCC 13032 was transformed with pPREx2 or pPREx2-IolG-Strep via electroporation as described previously (Eggeling and Bott, 2005) and the recombinant strains were grown on BHIS agar plates containing 25 µg/mL kanamycin.

2.4 Production of cutinase and GFP.

BHIS cultures of *C. glutamicum* cells harboring the different recombinant plasmids for the production of cutinase or GFP (Table 1) were grown overnight in a FlowerPlate (m2p-labs, Aachen, Germany) in a Microtron (Infors HT, Einsbach, Germany) at 900 rpm and 30 °C. Next, 50 µL of the respective cultures were transferred to FlowerPlate wells containing 800 µL CgIII medium (Menkel et al., 1989) supplemented with 2% (w/v) glucose, and growth was continued for an additional 6 h. Hereafter, 50 µL of the CgIII cultures were transferred to wells containing 800 µL CgXII minimal medium (Keilhauer et al., 1993) supplemented with 1% (v/v) glucose

and growth was continued overnight. The next day, the optical density of the CgXII cultures was determined by measuring the OD_{600}. The CGXII cultures were then used to inoculate fresh CgXII minimal medium containing 1% (v/v) glucose at an OD_{600} of 0.5 in a new FlowerPlate.

Cells were then cultivated in a BioLector system (m2p-labs, Aachen, Germany) equipped with a GFP filter module (λ_{ex} 488 nm, λ_{em} 520 nm) at 30 °C, 1200 rpm and 85% relative humidity. Bacterial growth was monitored online by measuring backscatter at 620 nm. After 3 - 4 h, gene expression was induced by the addition of isopropyl-β-D-thiogalactopyranoside (IPTG) in case of pEKEx2-derived plasmids and anhydrotetracyclin (ATc) in case of pCLTON1-derived plasmids, at indicated final concentrations and cultivation was continued overnight. During cultivation, FlowerPlates were always covered with a sterile gas permeable membrane. In case of *gfp* expression, the GFP fluorescence (signal gain factor 90) and biomass development (backscatter, signal gain factor 20) were monitored in parallel. The specific GFP fluorescence was obtained by dividing the GFP fluorescence (AU) by the corresponding backscatter (AU) and then plotted against time. Finally, data were fitted using the following logistic fit function in OriginPro:

$$y = \frac{A1 - A2}{1 + (x/x0)^p} + A2$$

Herein, y represents the specific GFP fluorescence value at a given inducer concentration, x. *A*1 and *A*2 represent the minimum and maximum specific fluorescence, respectively, while p is the exponent. The derived parameter x0 represents the EC_{50}, i.e. the half maximal effective inducer concentration (the inducer concentration at which 50% of its maximal effect is observed).

2.5 SDS-PAGE and Western blot analysis.

After cultivation, the OD_{600} of the cultures was determined (typically OD_{600} ~15) and the culture medium and *C. glutamicum* cells were separated by centrifugation. In case of secretory protein

production of cutinase, 500 µL of the culture supernatants were supplemented with 60 µL 100% (w/v) trichloroacetic acid (TCA) solution prepared in ddH_2O. Proteins were allowed to precipitate for at least 1 h at 4 °C and then sedimented by centrifugation for 30 min at 20,000*g* and 4 °C. The supernatants were removed and the pellets were dissolved in 100 µL 1x sample buffer (Laemmli, 1970). The pH was adjusted by adding 12 µL of a 1 M Tris solution (pH ~11.5). For each protein sample, equal amounts corresponding to 1.5 OD_{600} cell equivalents were analyzed by 12.5% SDS-PAGE (Green and Sambrook, 2012). In case of cytosolic protein production, cells were washed and resuspended in lysis buffer (30 mM Tris-HCl pH 8 for GFP or 100 mM Tris-HCl pH 7.5, 1 mM $MgSO_4$ for IolG) and disrupted using 0.1 mm zirconia/silica beads (BioSpec Products Inc., Bartlesville, USA) in a MM2 mixer mill (Retsch GmbH, Haan, Germany). Whole cell lysates were cleared by centrifugation at 13,000*g* and 4 °C for 20 min. Equal amounts of protein (10 µg per lane) were analyzed by SDS-PAGE and Western blotting according to standard procedures (Green and Sambrook, 2012). Proteins were visualized by Coomassie Brilliant Blue staining or immunodetection, repectively. For immunodetection of GFP, a polyclonal anti-GFP antibody was used as described previously (Lausberg et al., 2012), while for IolG-Strep a Strep-Tactin-HRP conjugate (IBA Lifesciences, Göttingen, Germany) was used.

2.6 Cutinase activity assays.

Cutinase activity in culture supernatants was determined by a spectrophotometric assay, using *p*-nitrophenyl palmitate (pNPP) as a substrate, essentially as described previously (Caspers et al., 2010). In brief, supernatants were 30-fold diluted in 66.5 mM Sørensen's phosphate buffer pH 8.0. Next, 20 µL of the diluted supernatants were transferred to a standard 96-well microtiter plate (mtp), while 20 µL of Sørensen's buffer served as control. For every mtp, reagent was freshly prepared by mixing 1 volume of 30 mg pNPP dissolved in 10 mL isopropanol with 9 volumes of Sørensen's buffer containing 1.11 mg/mL gum arabic and 2.3 mg/mL sodium deoxycholate. The enzymatic reaction was started by rapid addition of 180 µL reagent to each

well using a multichannel pipette. The mtp was then transferred to a plate reader (Tecan Deutschland GmbH, Crailsheim, Germany) preheated at 37 °C. After brief and vigorous mixing, the absorbance at 410 nm was measured for 15 min at 1 min intervals. The cutinase activity was then calculated from the linear slope using a molar extinction coefficient of 15,000 $M^{-1}cm^{-1}$ (Caspers et al., 2010).

In addition, cutinase production was visualized through means of an *in situ* activity assay on agar plates. For this purpose, *C. glutamicum* cells were transformed with pEKEx2-NprE-cutinase or pPBEx2-NprE-cutinase plasmid and plated on BHIS agar plates containing 25 µg/mL kanamycin. Plates were incubated for 2 days at 30 °C. Transformants were then picked and cultivated separately in 500 µL $BHIS_{kan}$ in 2 mL Eppendorf tubes for 5 h at 30 °C and 250 rpm. Next, 5 µL of the different cultures were spotted on $BHIS_{kan}$ agar plates containing 100 µM IPTG for induction of cutinase expression and 1% (v/v) Tween-20, which serves as a substrate for cutinase (Ramnath et al., 2017). The plates were incubated for 2 days at 30 °C. The formation of optically turbid zones was indicative for the formation of enzymatically active cutinase.

2.7 Strep-Tactin affinity chromatography.

Cell pellets were suspended in lysis buffer containing 100 mM Tris-HCl pH 7.5, 200 mM NaCl, 5% (v/v) glycerol and cOmplete EDTA-free protease inhibitor (Roche) using 4 mL per g wet cell weight. The cells were lysed by five passages through a French Press at 18,000 psi. The resulting cell extract was first centrifuged at 5,000*g* and 4 °C for 20 min and the supernatant was then subjected to ultracentrifugation at 45,000*g* and 4 °C for 1 h. The resulting supernatant was incubated with avidin (25 µg/mg protein) for 30 min on ice before applying it on a Strep-Tactin gravity flow affinity column with a bed volume of 3 mL (IBA Lifesciences, Göttingen, Germany). The column was washed with 5 x 3 mL lysis buffer and bound protein was eluted in 5 x 1.5 mL fractions using elution buffer consisting of 100 mM Tris-HCl pH 7.5, 200 mM

297 NaCl, 5% (v/v) glycerol, 2.5 mM desthiobiotin and cOmplete EDTA-free protease inhibitor. The
298 elution fractions were analyzed by SDS-PAGE.

299

300 **2.8 *Myo*-inositol dehydrogenase activity assays.**

301 *Myo*-inositol dehydrogenase activity was determined in a spectrophotometric assay by
302 measuring the absorbance increase at 340 nm in an assay mixture containing 2 mM NAD^+ and
303 50 mM *myo*-inositol. Cell-free extracts (see section 2.7) were diluted in reaction buffer (100
304 mM Tris-HCl, pH 7.5, 1 mM $MgSO_4$). For activity assays with purified protein, elution buffer
305 was exchanged for reaction buffer using PD-10 columns (GE Healtcare Life Sciences)
306 according to the supplier's manual. Diluted protein was pre-incubated with 2 mM NAD^+ in a
307 volume of 450 µL at 30 °C in a plastic semi-micro cuvette (Sarstedt). After 30 sec the reaction
308 was started by the addition of 50 µL of a 500 mM *myo*-inositol solution and the absorbance
309 increase at 340 nm and 30 °C was measured for 4 min using a Jasco V560 spectrophotometer.
310 For calculation of the specific activity an extinction coefficient of 6.3 mM^{-1} cm^{-1} for NADH was
311 used. Background NADH formation was measured without addition of *myo*-inositol and
312 subtracted from the activities determined in the presence of *myo*-inositol.

313

314

3. Results and discussion

3.1 Construction of the *C. glutamicum* expression vector pPBEx2.

The *E. coli/C. glutamicum* shuttle vector pEKEx2 is an IPTG-inducible expression vector (Eikmanns et al., 1994) that has been used successfully in many different laboratories for the production of cellular and secretory proteins by *C. glutamicum,* for more than two decades now. Less favorable however, can be the leaky gene expression in the absence of the inducer that is generally associated with pEKEx2-derived plasmids (Goldbeck and Seibold, 2018; Jurischka et al., 2020; Kortmann et al., 2015; Lausberg et al., 2012). We now re-examined the published nucleotide sequence of pEKEx2 (GenBank: AY585307.1) and found that the plasmid contains a modified DNA coding region for the repressor LacI (*lacI**). The altered DNA sequence codes for a LacI derivative with an incorrect extended C-terminus (Fig. 1A and B), which likely contributes to reduced function of the repressor. However, distant from the modified *lacI* gene, the pEKEx2 backbone contains a stretch of DNA that actually corresponds to a correct LacI C-terminal coding sequence (Fig. 1A, C-*lacI*). Further inspection of this DNA region revealed two sites of duplicated DNA sequences (Fig. 1A). Herein, 1109-1142 bp were found to be identical to the *lacI** region immediately preceding the incorrect 3'-end (i.e. 6729-6762 bp), while 930-968 bp (reverse complement) constitute an incomplete *tacI* promotor consisting only of the *lac* operator and the ribosome binding site (*rbs*) (Fig. 1A).

DNA sequencing of the pEKEx2 plasmid available in our laboratory confirmed that it is identical to the published nucleotide sequence (GenBank: AY585307.1) and thus contains both the modified *lacI** and the aforementioned duplicate DNA sequences. From molecular genetic studies of *E. coli* in particular it is known that rearrangements can occur between repeated DNA sequences, which in turn can lead to either deletion or duplication of genetic material flanked by the sequence repeats (Bzymek and Lovett, 2001). The duplicate sequences within pEKEx2 region 930-1142 are unnecessary and may contribute to plasmid instability (see below section 3.2). Moreover, LacI is likely to bind also to the superfluous duplicate *lac* operator site in pEKEx2, thereby effectively reducing the amount of repressor molecules available for

binding to the primary *lac* operator that controls target gene transcription and thus contributing to the leaky gene expression observed for pEKEx2 plasmids. We therefore decided to eliminate these unfavorable properties of pEKEx2, using standard PCR along with Gibson DNA assembly (see section 2.3 and Table 2). In such manner, the pEKEx2-derivative pPBEx2 was constructed which harbors a correct *lacI* gene and which lacks the parental DNA region 930-1140 bp (Fig. 1).

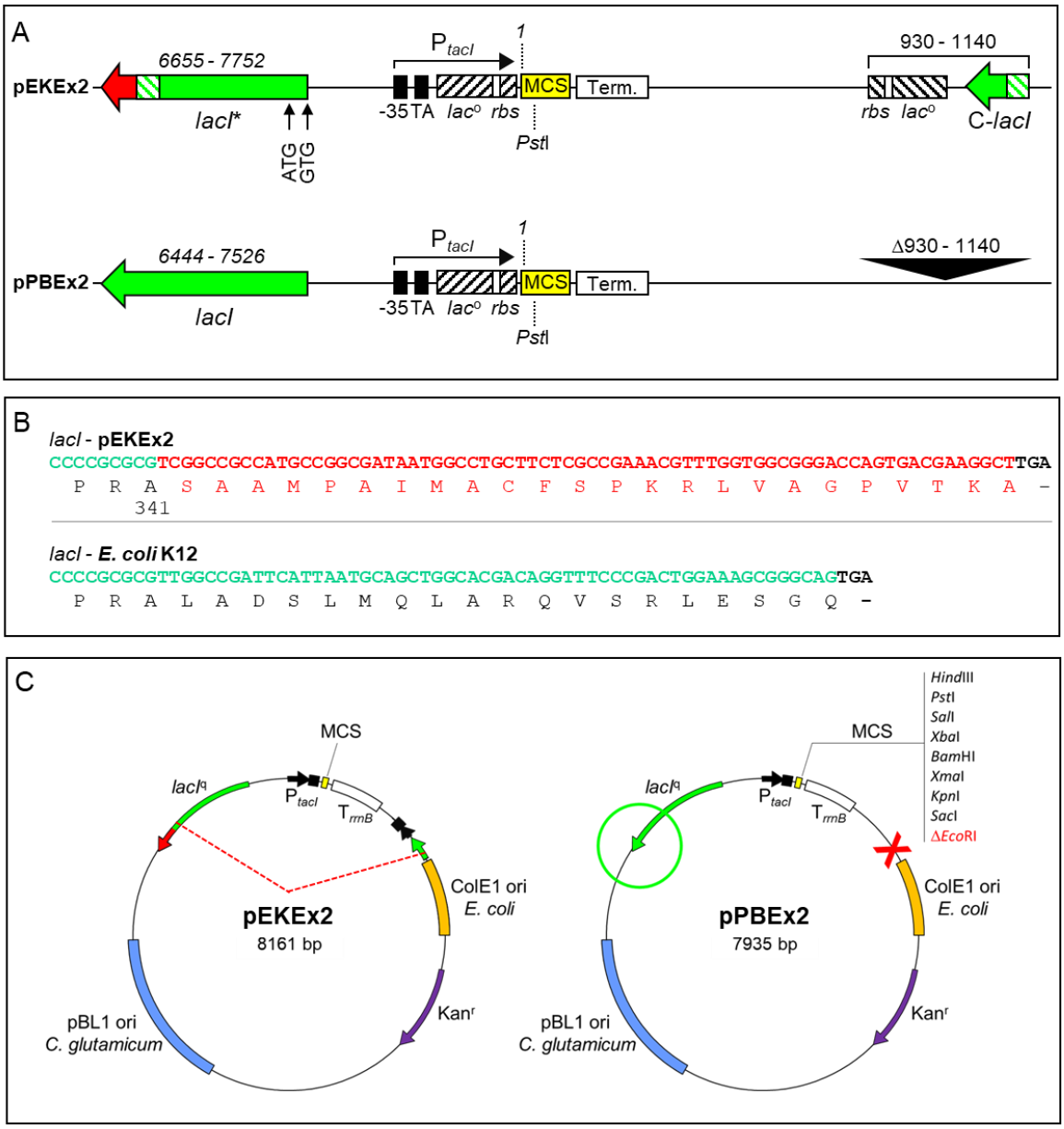

Fig. 1. Properties of expression vector pPBEx2. A plasmid map was generated from the DNA sequence of pEKEx2 (GenBank: AY585307.1), with the starting position at the first base of the *Hind*III site within the MCS. (A) Schematic view of relevant properties of pEKEx2 (upper) and its cured derivative pPBEx2 (lower). The *lacI*^{q} allele of pEKEx2 encodes a LacI repressor (*lacI**) with a modified C-terminus (indicated by red arrow). The 5'-end of *lacI**

was found to be correct, but the start codon was incorrectly assigned (ATG); the actual start codon (GTG) is located 41 codons more upstream. Notably, pEKEx2 region 930-1140 actually harbors a DNA sequence identical to a proper LacI C-terminal coding region (C-*lacI*). Moreover, within region 930-1140 DNA sequences were identified that are identical to (i) the *lac* operator (lac^O) and ribosome binding site (*rbs*) of the *tacI* promoter (reverse complement; indicated by black dashed boxes) and (ii) to the *lacI** region immediately preceding the modified 3'-end (indicated by green dashed boxes). (B) Comparison of the C-terminal coding regions of the *lacI* gene from expression vector pEKEx2 and from *E. coli* K12. The incorrect C-terminal tail of the pEKEx2-encoded repressor starts after Ala341. (C) Plasmid maps of expression vector pPBEx2 (right) and its parent pEKEx2 (left). pPBEx2 harbors a correct $lacI^q$ allele and a complete deletion of pEKEx2 region 930-1140 bp. For in-house cloning purposes, the *Eco*RI restriction site of the parental MCS was eliminated in pPBEx2. The dashed red lines (pEKEx2) mark the *lacI* twin sequences that may facilitate excision of the DNA fragment in-between via homologous recombination events (see below, section 3.2). The DNA sequence of pPBEx2 was deposited in NCBI and is available under the GenBank accession number MT670349.

3.2 pPBEx2 exhibits tight gene repression in the absence of inducer along with improved plasmid stability.

To assess the performance of the novel expression vector pPBEx2, first the secretory production of the model enzyme cutinase from *Fusarium solani pisi* was studied in *C. glutamicum* (Fig. 2). To enable secretion, the cutinase carried the N-terminal Sec signal peptide of the neutral protease NprE from *Bacilllus subtilis*. Consistent with previous reports (Hemmerich et al., 2019; Jurischka et al., 2020) pEKEx2-NprE-cutinase facilitated high-level secretory production of cutinase (Fig. 2). But notably, in the absence of IPTG already a considerable amount of cutinase is detected in the culture medium as evidenced by cutinase activity measurements (Fig. 2A) and SDS-PAGE analysis (Fig. 2B). Non-induced cells carrying pEKEx2-NprE-cutinase produced ~1100 U/L cutinase, which constitutes nearly 29% of the cutinase activity achieved at saturating amounts of IPTG, i.e. ~3800 U/L at 2.5 mM IPTG. Clearly, under non-induced conditions substantial cutinase expression had occurred. In contrast, virtually no cutinase was present in the culture supernatants of non-induced cells harboring pPBEx2-NprE-cutinase (Fig. 2). In this case, less than 50 U/L were measured, which

is ~22-fold lower than the activity observed with pEKEx2-NprE-cutinase under identical conditions. Nevertheless, at full induction (2.5 mM IPTG) both the amount and the activity of the secreted cutinase produced from pPBEx2 were similar to those achieved with pEKEx2, which indicates that pPBEx2 is an excellent alternative to pEKEx2 for high-level secretory production of cutinase by *C. glutamicum*. Importantly, the expression of cutinase from pPBEx2 appears to be stringently controlled by the inducer IPTG, which indicates successful restoration of repressor (LacI) functionality.

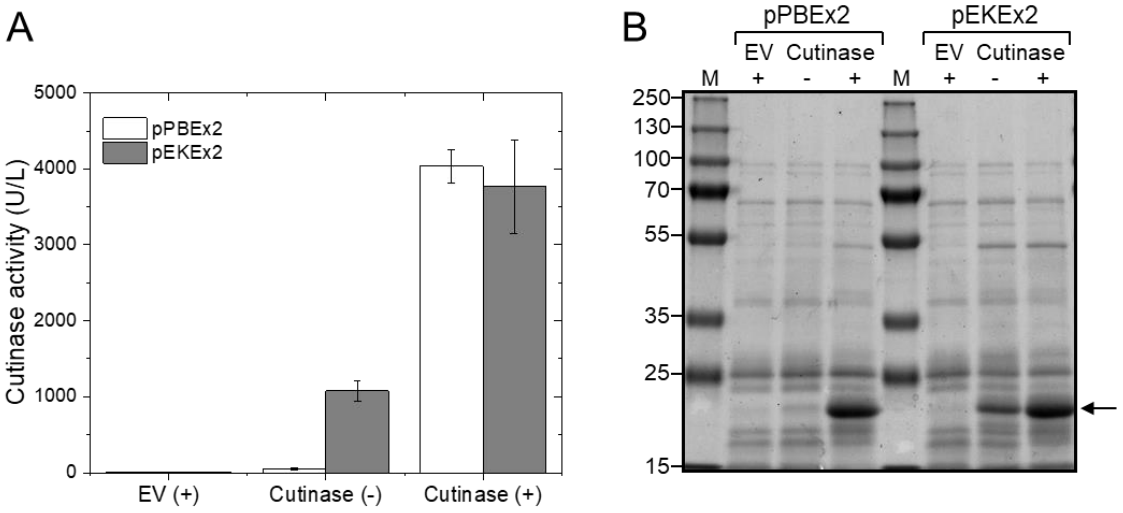

Fig. 2. Secretory production of cutinase using expression vectors pPBEx2 and pEKEx2. *C. glutamicum* K9 cells harboring pPBEx2-NprE-cutinase, pEKEx2-NprE-cutinase or the corresponding empty vector controls (EV) pPBEx2 and pEKEx2 were grown at 30 °C at 1200 rpm in a BioLector system as described in section 2.4. Four hours after inoculation, either water (-) or IPTG (+; 2.5 mM final concentration) was added to the cultures and bacterial growth was continued overnight. Culture supernatants were then analyzed with respect to cutinase activity and amount. (A) Cutinase activity was determined by a photometric assay as described in section 2.6. Results for cells harboring the respective pPBEx2- or pEKEx2-derived plasmids are shown as white and gray bars, respectively. Mean values from three biological replicates and corresponding standard deviations are indicated. (B) Cutinase protein in the culture supernatants was analyzed by 12.5% SDS-PAGE and visualized by Coomassie Brilliant Blue staining. M, marker proteins with molecular masses indicated in kDa. The arrow indicates the position of cutinase (20.7 kDa).

Previous studies on gene expression in *C. glutamicum* at the single cell level using fluorescence activated cell sorting (FACS) revealed that cells carrying pEKEx2-eyfp plasmid exhibit considerable leaky gene expression in the absence of inducer, while after induction with IPTG, a substantial heterogeneity of eYFP fluorescence was apparent within the *C. glutamicum* population (Kortmann et al., 2015). It was proposed that the heterogeneity in eYFP synthesis was caused by instability of the pEKEx2-eyfp plasmid, which in turn, likely originated from vector determinants unrelated to target gene expression (e.g. the pBL1 replicon). We noticed heterogeneity of transformants also in case of electroporation of the pEKEx2-NprE-cutinase plasmid (isolated from *E. coli*) into *C. glutamicum*. Typically, when single transformants were screened for cutinase production by spotting them on Tween-20-containing agar plates, a significant, but variable, number of transformants was unable to produce cutinase. The results of an exemplary experiment are shown in Fig. 3A. In this case, 15 of the 24 spotted transformants did not produce cutinase.

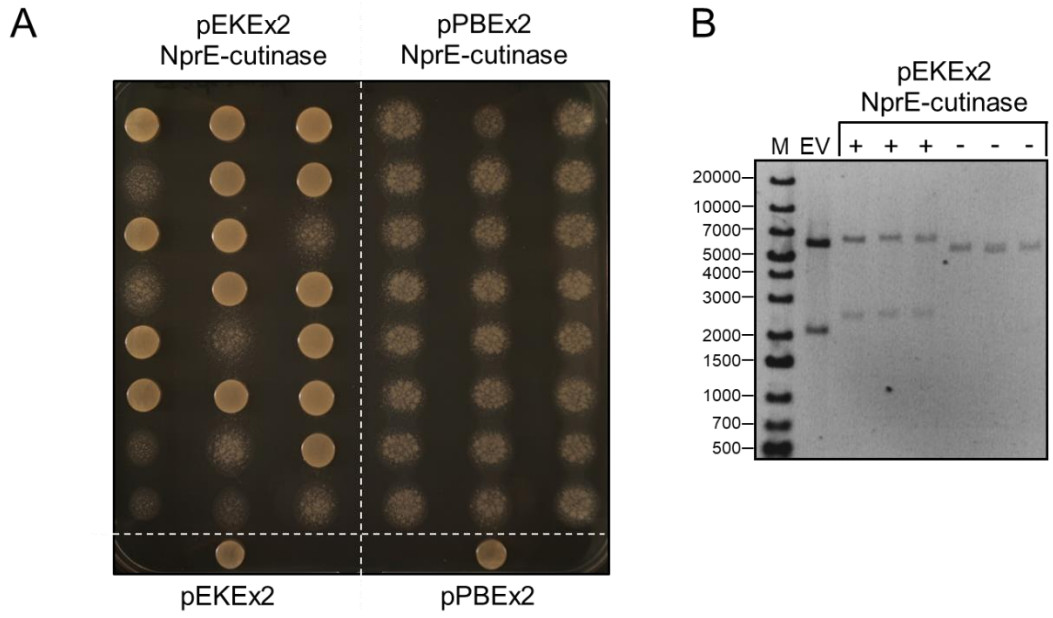

Fig. 3. Heterogeneity of *C. glutamicum* cells transformed with pEKEx2-NprE-cutinase. (A) Analysis of cutinase production by *C. glutamicum* cells transformed with pEKEx2-NprE-cutinase (left), pPBEx2-NprE-cutinase (right), or the corresponding empty vectors pEKEx2 or pPBEx2 (bottom). After transformation, single colonies were picked and grown for 5 h in 500 µL $BHIS_{kan}$ medium as described in section 2.6. Next, 5 µL of the cultures were spotted

on a $BHIS_{kan}$ agar plate containing 100 µM IPTG for cutinase expression and 1% (v/v) Tween-20 as the substrate for cutinase. The plate was then incubated for 2 days at 30 °C. Cutinase-producing clones are characterized by a patchy growth phenotype and optically turbid zones. (B) Restriction analysis of plasmids isolated from three different *C. glutamicum* clones exhibiting either the cutinase producing (+) or non-producing (-) phenotype. The empty vector pEKEx2 (EV) served as restriction control. M, GeneRuler DNA ladder (in bp). Plasmids were digested with *Kpn*I and *Xho*I. *Kpn*I cleaves in the MCS of pEKEx2 (EV) or inside the cutinase gene of pEKEx2-NprE-cutinase, whereas *Xho*I cleaves in the backbone of both respective plasmids. Restriction mixtures were analyzed by agarose gel electrophoresis and DNA was visualized by ethidium bromide staining. Expected fragments for pEKEx2 (8161 bp): 2131 and 6030 bp, and for pEKEx2-NprE-cutinase (8883 bp): 2506 and 6377 bp. Note that *Kpn*I-*Xho*I-treatment of plasmids isolated from producer clones exhibited the two expected fragments, whereas the plasmids from non-producer clones yielded only a single fragment of ~6 kb.

Subsequent restriction analysis of plasmids isolated from *C. glutamicum* clones that were unable to produce cutinase revealed that they lack about 3 kb in comparison to the plasmids isolated from cutinase-producing clones (Fig. 3B). Similarly aberrant pEKEx2-NprE-cutinase plasmids were also recovered from *E. coli* transformants (unpublished results). Notably, when correct pEKEx2-NprE-cutinase plasmid isolated from *C. glutamicum* was re-transferred into *C. glutamicum,* heterogeneity of transformants was not evident (unpublished results), which suggests that the excision of the 3 kb fragment from pEKEx2-NprE-cutinase most likely originates in the cloning host *E. coli*. Complete DNA sequencing of one of these aberrant plasmids revealed that a 3.2 kb DNA fragment was lacking. Strikingly, the deletion started from within the *lacI** gene at the site immediately preceding the modified 3'-end and ended immediately after the duplicate *lacI* sequence within pEKEx2 region 930-1140 (Fig. 1A and C), and thus the entire promoter region and cutinase gene were lacking (Fig. 1A). Obviously, loss of the promoter region and the cutinase gene explains the non-producer phenotype of the corresponding *C. glutamicum* transformants (Fig. 3A). It is of note that such truncated plasmids would still be able to propagate, as the bacterial replicons (*E. coli* and *C. glutamicum)* and the kanamycin resistance gene are intact (Fig. 1C). Since in the pEKEx2-NprE-cutinase plasmid the 3.2 kb fragment is flanked by identical *lacI*-derived DNA sequences (Fig. 1A and C), it seems plausible that the *lacI* twin sequences are able to facilitate DNA rearrangements leading

to excision of the 3.2 kb fragment in-between. At present, the exact underlying molecular mechanism of the deletion remains unknown. However, since the deletion had occurred in *E. coli* XL1-blue cells, which carry the *recA1* mutation (Table 1), it seems likely that the aforementioned homology-dependent recombination events can take place in a RecA-independent manner.

We speculate that the loss of the cutinase fragment in *E. coli* might be promoted by cellular toxicity of the active cutinase. Cutinase possesses phospholipase activity (Parker et al., 2007) and it has been demonstrated that cutinase expression in *E. coli* can alter the membrane permeability and even disrupt the cell envelope (Su et al., 2013). The cellular toxicity of cutinase may thus favor the selection of *E. coli* cells that do not produce the cutinase. Moreover, such occurrence is likely to be facilitated by the substantial leakiness of the pEKEx2 promoter (due to the defective LacI) and the presence of identical flanking DNA sequences that allow excision of the cutinase gene. In contrast, target gene expression from the pPBEx2 plasmid is tightly repressed in the absence of inducer (Figs. 2 and 4) and pPBEx2 is devoid of unfavorable duplicate DNA sequences, as it lacks the parental region 930-1140. Importantly, following electroporation of the pPBEx2-NprE-cutinase construct (isolated from *E. coli*) into *C. glutamicum*, all transformants are able to produce cutinase in the presence of IPTG (Fig. 3A). The lack of heterogeneity of the transformants indicates improved plasmid stability of the pPBEx2-NprE-cutinase construct in comparison to its counterpart pEKEx2-NprE-cutinase.

3.3 Expression vector pPBEx2 allows tight regulation of GFP synthesis.

To characterize the expression vector pPBEx2 in more detail, also the production of a cytosolic protein was investigated. For this purpose, GFP was chosen as a reporter protein, as its fluorescence can be conveniently monitored during cultivation. Expression of *gfp* from pPBEx2 in *C. glutamicum* was compared to that from the parental vector pEKEx2 and the previously described anhydrotetracycline (ATc)-inducible expression vector pCLTON1 (Lausberg et al., 2012). To this end, *C. glutamicum* cells harboring either pPBEx2-GFP, pEKEx2-GFP or

pCLTON1-GFP were induced with the appropriate inducer to different final concentrations as indicated, and the fluorescence development was measured over time. Cells carrying the corresponding empty vectors served as controls. In Fig. 4A the specific fluorescence is plotted against time for selected cultures as indicated.

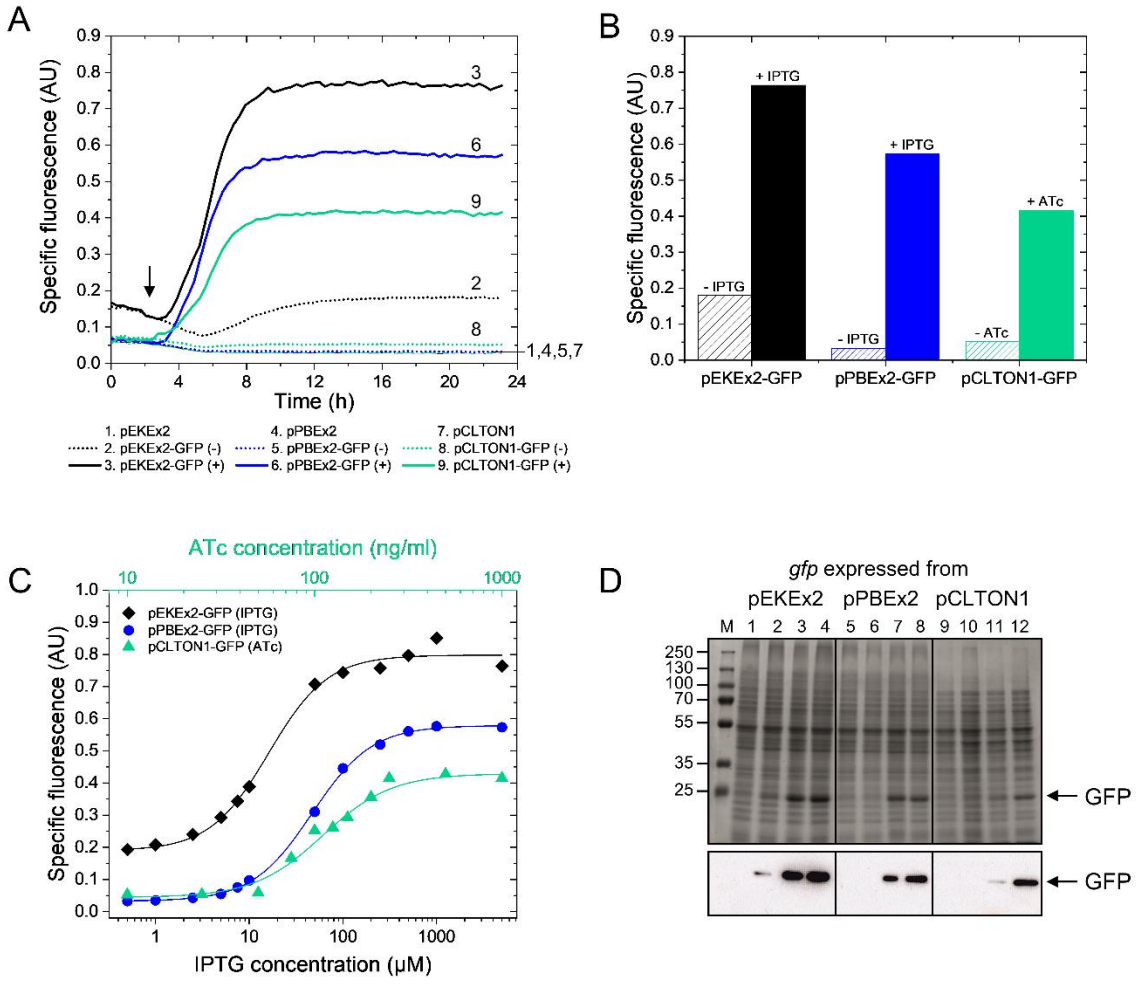

Fig. 4. Analysis of GFP synthesis by *C. glutamicum* in dependence of the inducer concentration. *C. glutamicum* cells harboring pEKEx2-GFP, pPBEx2-GFP, pCLTON1-GFP, or the corresponding empty vector controls pEKEx2, pPBEx2 and pCLTON1 were grown at 30 °C and 1200 rpm in a BioLector, and the bacterial growth (backscattered light) and the GFP fluorescence were measured online. After 3 h, the inducer (IPTG or ATc) was added to the respective cultures and growth was continued overnight. In case of pEKEx2 (black curves) and pPBEx2 (blue curves) the final IPTG concentration ranged from 0 - 5 mM, while for pCLTON1 (green curves) the anhydrotetracycline (ATc) concentration ranged from 0 - 1 µg/mL. (A) The development of the specific fluorescence over time is shown for cells that were not induced (-, curves 2, 5, 8), induced with maximum inducer concentration (+, curves 3, 6, 9) and cells harboring the corresponding empty vector controls (curves 1, 4, 7). The arrow indicates the time point of induction at which the inducer (IPTG or ATc) was added. (B) Comparison of the specific

fluorescence levels at the end of the cultivation achieved with the different expression plasmids as indicated. Results are shown for non-induced cells and cells that were induced with maximum amount of inducer (5 mM IPTG or 1 µg/mL ATc). (C) The specific fluorescence at the end of the cultivation is plotted in dependence of the inducer concentration for cells expressing *gfp* from pEKEx2 (black diamonds), pPBEx2 (blue circles) and pCLTON1 (green triangles). The data were fitted using a logistic fit function in OriginPro as described in section 2.4. (D) SDS-PAGE (upper panel) and Western blot (lower panel) analysis of total cell lysates at the end of the cultivation. Proteins were visualized by Coomassie Brilliant Blue staining and immunodetection using a GFP-specific antibody, respectively. Results are shown for cells expressing *gfp* from indicated plasmids at different inducer concentration. In case of pEKEx2 and pPBEx2, results for 0, 50 and 250 µM IPTG are shown in lanes 2-4 and 6-8, respectively. For pCLTON1, results for 0, 100 and 1000 µM ATc are shown in lanes 10-12, respectively. Analysis of cell lysates of non-induced cells harboring the corresponding empty vectors are shown in lanes 1, 5 and 9.

In all cases, cells carrying plasmid-borne *gfp* exhibited, shortly after inducer addition, a sharp increase in specific fluorescence, which plateaued after approximately 8 h of cultivation (Fig. 4A). Notably, in case of pEKEx2-GFP the specific fluorescence at the end of the cultivation of non-induced cells (0.18 AU) was considerably higher than that of the corresponding empty vector control cells (0.03 AU), which indicates that a substantial amount of GFP was produced even in the absence of IPTG (Fig. 4A, *cf*. 2 and 1 and Fig. 4B). These results are in full agreement with previous observations (Lausberg et al., 2012) and once more demonstrate that the pEKEx2 plasmid exhibits substantial promoter leakiness. In contrast, non-induced cells carrying pPBEx2-GFP did not exhibit significant GFP fluorescence (Fig. 4A and 4B). In fact, the specific fluorescence levels of the respective cells were identical to those of cells carrying the empty vector pPBEx2, i.e. 0.03 AU (Fig. 4A, *cf*. 5 and 4). Thus in case of pPBEx2, expression of *gfp* was tightly repressed in the absence of the inducer IPTG, which indicates that the pPBEx2-encoded repressor LacI is fully functional. A similarly stringent control of *gfp* expression was observed for the ATc-inducible pCLTON1 (Fig. 4A. *cf*. 7 and 8), as has also been described previously by Lausberg et al. (2012). Consistent with the GFP fluorescence measurements, SDS-PAGE and Western blot analysis revealed no GFP in the lysate of non-induced cells harboring either pPBEx2-GFP or pCLTON1-GFP (Fig. 4D, lanes 6 and 10,

524 respectively), whereas GFP was clearly present in the lysate of non-induced cells carrying
525 pEKEx2-GFP (Fig. 4D, lane 2).

526 By plotting the specific (GFP) fluorescence at the end of the cultivation in dependence of the
527 inducer concentration, typical sigmoidal dose-response curves were obtained for the three
528 different expression vectors (Fig. 4C). Notably, whereas in case of pPBEx2 ~500 µM IPTG is
529 required to achieve full induction of *gfp* expression, considerably less IPTG is required in case
530 of pEKEx2, i.e. ~250 µM. In addition, the EC_{50} values, *i.e.* the effective inducer concentration
531 at which 50% of the maximum specific GFP fluorescence is achieved, differed markedly: 47
532 µM IPTG in case of pPBEx2 and 16 µM IPTG in case of pEKEx2. Analysis of the dose-
533 response of the anhydrotetracycline (ATc)-inducible expression vector pCLTON1 revealed an
534 EC_{50} of 110 ng/mL ATc for *gfp* expression, while full induction is achieved at ~250 ng/mL ATc,
535 which is in agreement with previous observations (Lausberg et al., 2012).

536 The differences in dose-response observed between pEKEx2 and its offspring pPBEx2 likely
537 reflect differences in the behavior of the different LacI repressor proteins encoded by the
538 respective plasmids. Overall the data suggest that the pEKEx2-borne repressor, which carries
539 a modified C-terminus (Fig. 1A), exhibits reduced functionality in comparison to its native
540 counterpart produced from pPBEx2, but nevertheless is still able to functionally interact with
541 the inducer IPTG (Figs. 2 and 4). The ~3-fold lower EC_{50} in case of *gfp* expression may indicate
542 an altered affinity of the modified repressor toward IPTG and/or *lac* operator site. In this
543 respect, it is interesting to note that the C-terminus of LacI is important for oligomer formation.
544 Herein, the C-terminal residues Pro339 - Gln360 encompass an α-helix that facilitates LacI
545 tetramer formation (Chakerian et al., 1991; Chen and Matthews, 1992; Stenberg and Vihinen,
546 2009). Since the pEKEx2-encoded LacI lacks the native C-terminal residues Leu342 - Gln360,
547 the structural determinants that are required for tetramerization are no longer present.
548 Moreover, deletions or point mutations in the Pro339 - Gln360 region are known to result in
549 dimeric repressors that exhibit IPTG-binding properties similar to those of the wild-type
550 tetrameric repressor, while the apparent binding affinity for the *lac* operator is reduced
551 (Chakerian et al., 1991; Chen and Matthews, 1992). Since the operator dissociation rate

552 constants of such mutant dimeric LacI proteins and wild-type tetrameric LacI were comparable,
553 the diminished apparent binding affinity has been attributed to differences in the association
554 process, and most likely relates to increased dissociation of the dimer into monomers, which
555 are incapable of DNA-binding (Chakerian et al., 1991; Chen and Matthews, 1992). Taken
556 together it seems plausible that the pEKEx2-encoded LacI with modified C-terminus is
557 functional as a dimer rather than tetramer.

558 Finally, taking the specific fluorescence at the end of the bacterial cultivation achieved at
559 maximum inducer concentration as a measure for the maximum amount of GFP produced (Fig.
560 4B), and taking into account the general background fluorescence (empty vector controls: 0.03
561 AU), the performance of the three different expression vectors followed the order: pEKEx2
562 (0.73 AU) > pPBEx2 (0.54 AU) > pCLTON1 (0.39 AU). The maximum levels of GFP achieved
563 with pEKEx2 thus were significantly higher than those achieved with its derivative pPBEx2.
564 The exact cause for this effect remains obscure. However, it is plausible that the functional
565 differences of the respective plasmid-encoded LacI repressor proteins contribute to this
566 phenomenon. One might speculate that even in the presence of the maximum amount of IPTG,
567 an equilibrium exists in which a certain amount of the intact LacI repressor encoded by pPBEx2
568 is in its IPTG-free form and binds with high affinity to the *lac* operator. In contrast, the lower
569 affinity of the partially defective LacI from pEKEx2 for the *lac* operator would lead to a lower
570 proportion of repressed *lac* operator sites under fully induced conditions, and therefore to
571 higher final amounts of GFP. Nevertheless, pEKEx2 and its cured derivative pPBEx2 both
572 clearly outperformed the tightly controlled pCLTON1 in terms of the GFP production level.

573

574 **3.4 Construction of the *C. glutamicum* expression vector pPREx2.**

575 We previously reported the construction of the pEKEx2 derivative pAN6, which is characterized
576 by an altered multiple cloning site including a *C. glutamicum* consensus ribosome binding site
577 (Pfeifer-Sancar et al., 2013) upstream of a unique *Nde*I restriction site followed by a unique
578 *Nhe*I restriction site and a Strep-tag II-encoding sequence followed by a stop codon. In this

way, target genes can be cloned as *Nde*I-*Nhe*I fragments into pAN6 adding a Strep-tag II to the C-terminus of the target protein (Frunzke et al., 2008). Expression plasmids based on pAN6 were used in a variety of studies with *C. glutamicum*, e.g. for overproduction and purification of the transcriptional regulator FtsR (Kraxner et al., 2019). As the features of pAN6 proved to be useful in many applications, we transferred these features also into the newly constructed pPBEx2 vector. For this purpose, Gibson assembly was used based on three PCR fragments; one covering the multiple cloning site of pAN6 and two fragments covering large portions of pPBEx2. The oligonucleotides for PCR amplification of the latter two fragments were designed to destroy the unique *Nde*I site present in the pPBEx2 backbone (retained from its parent pEKEx2), as this site would interfere with *Nde*I-based cloning of target genes. The resulting expression plasmid was named pPREx2. A map of this vector is shown in Fig. 5 and the DNA sequence is available under GenBank accession number MT670350.

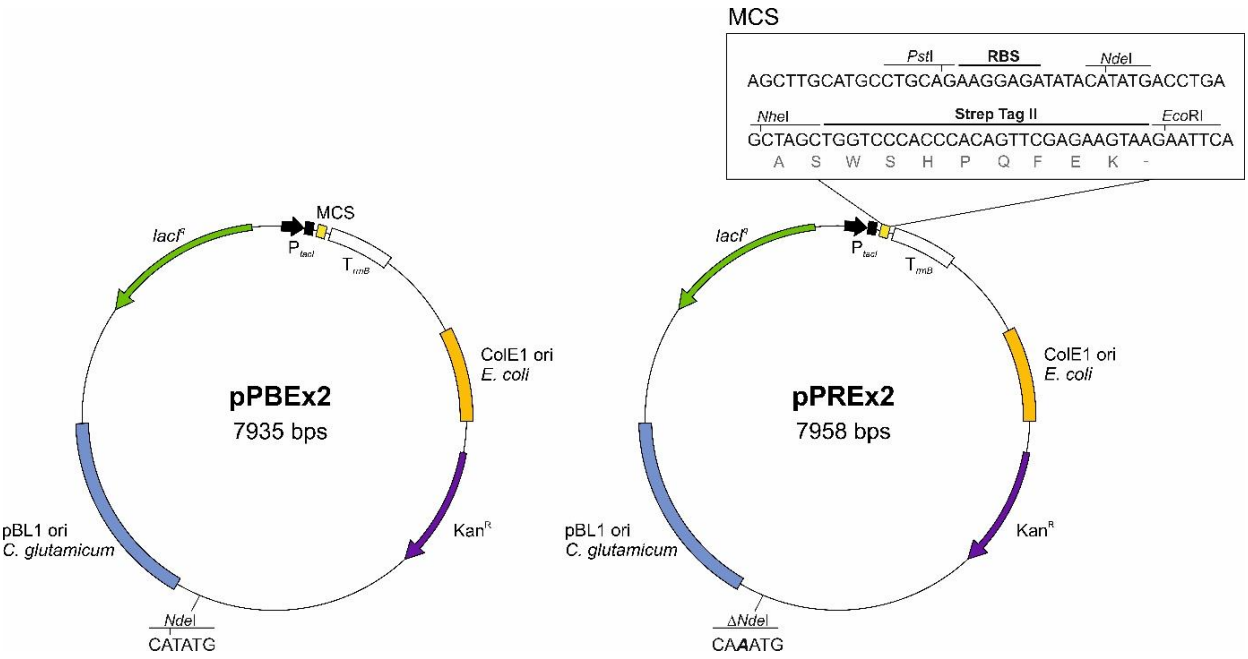

Fig. 5. Properties of expression vector pPREx2. Schematic drawing of expression vector pPREx2 (right) and its parent pPBEx2 (left). After the *rbs* of the P*tacI*, pPREx2 contains the multiple cloning site of pAN6 (Frunzke et al., 2008) with *Pst*I, *Nde*I, *Nhe*I, and *Eco*RI sites and the Strep-tag II-encoding sequence. A *C. glutamicum* consensus *rbs* (Pfeifer-Sancar et al., 2013) is located between the *Pst*I and *Nde*I site. The *Nde*I site in the pPBEx2 backbone was destroyed via a point mutation to enable cloning of target genes via *Nde*I into the MCS of pPREx2. Cloning of the target gene using *Nde*I-*Nhe*I allows in frame fusion of the corresponding target protein to the (C-terminal) Strep-tag II, while *Nde*I-*Eco*RI can be used if the Strep-tag is not desired.

3.5 Functionality of pPREx2.

To demonstrate the performance of pPREx2 in protein production in *C. glutamicum* and subsequent Strep-Tactin-based affinity purification, we amplified the *iolG* gene encoding *myo*-inositol dehydrogenase from genomic DNA of *C. glutamicum* (Krings et al., 2006) and cloned it into pPREx2 via Gibson assembly, resulting in plasmid pPREx2-IolG-Strep (see section 2.3.2). *C. glutamicum* wild-type was transformed with pPREx2-IolG-Strep or pPREx2 as negative control and cultured in shake flasks in BHI medium containing 2% (w/v) glucose and 25 µg/mL kanamycin at 130 rpm and 30 °C. For each recombinant strain two 100 mL cultures were inoculated to a starting OD_{600} of 0.5. When the cultures had reached an OD_{600} of 2.0, IPTG (1 mM final concentration) was added to one culture of each strain, whereas the second culture received an equal volume of water. The cultures were incubated for another 24 h, after which the cells were harvested and the soluble cell fractions were prepared as described in section 2.7. The soluble fractions were used for SDS-PAGE analysis and measurement of *myo*-inositol dehydrogenase activity. As shown in Fig. 6 (upper panel), a major protein band with an apparent mass of 37 kDa was visible in the sample of the culture with pPREx2-IolG-Strep that had received IPTG, whereas this protein appears to be absent in samples of the corresponding non-induced culture and control cultures carrying the empty vector pPREx2. Western blot analysis of IolG-Strep production confirmed the presence of the Strep-tag II and revealed that only a minute amount of IolG-Strep was produced in the absence of IPTG.

To establish if the produced IolG-Strep is active, *myo*-inositol dehydrogenase activity of the soluble cell fractions was determined using a spectrophotometric assay measuring NAD^+ reduction (see section 2.8). For the induced cells with pPREx2-IolG-Strep, a specific activity of 5.1 µmol min^{-1} (mg protein)$^{-1}$ was measured, while the activity for the non-induced cells was 0.12 µmol min^{-1} (mg protein)$^{-1}$, which was slightly higher than the activities found for the empty vector controls, 0.04 µmol min^{-1} (mg protein)$^{-1}$. These results indicate that IolG with C-terminal Strep-tag II is functional and confirms tight gene repression in the absence of IPTG, enabling a 43-fold increase in IolG activity after induction. The fact that only a very low IolG activity was detected in cultures containing the empty vector indicates that under the applied growth

conditions the *iolG* gene within the chromosomal *iol* gene cluster involved in *myo*-inositol uptake and degradation, is tightly repressed by the dedicated repressor IolR (Klaffl et al., 2013).

Next, the soluble cell fraction of the induced culture of *C. glutamicum* with pPREx2-IolG-Strep was used for purification of IolG-Strep by Strep-Tactin affinity chromatography (see section 2.7). As shown in Fig. 6, IolG-Strep could be successfully isolated and purified to near homogeneity. The specific activity of the purified protein was 27 µmol min^{-1} (mg protein)$^{-1}$, which is in the range found for purified *myo*-inositol dehydrogenases of other organisms, such as *Bacillus subtilis* (Ramaley et al., 1979) or *Klebsiella aerogenes* (Berman and Magasanik, 1966). Approximately 1.5 mg of purified IolG-Strep was obtained from 100 mL cell culture.

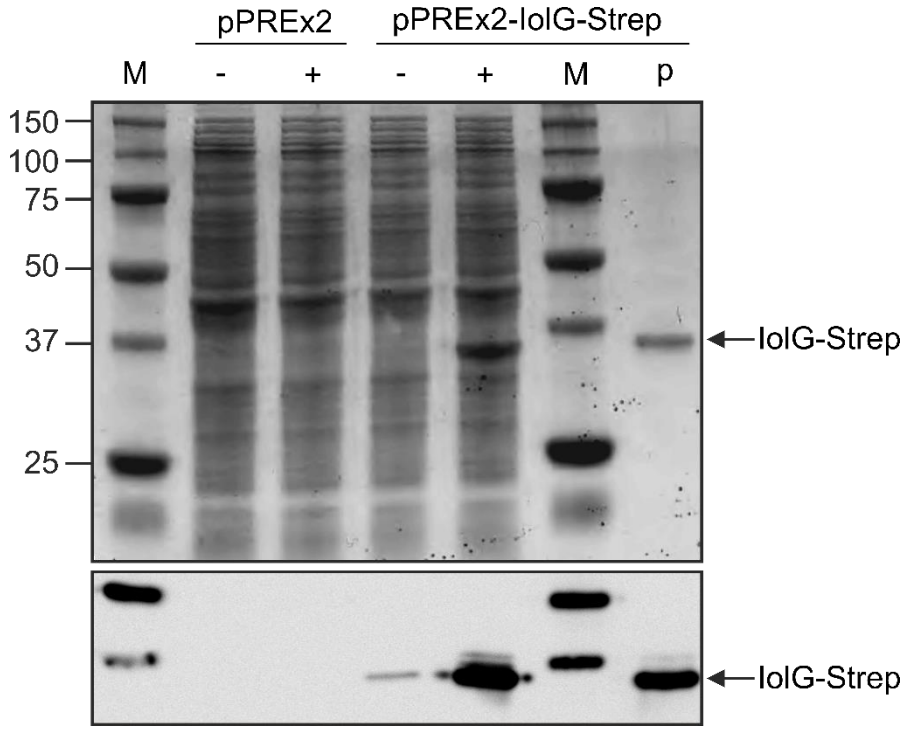

Fig. 6. Analysis of IolG-Strep overproduction in *C. glutamicum* and purification by Strep-Tactin affinity chromagraphy. Proteins were visualized by Coomassie Brilliant Blue staining after SDS-PAGE (upper panel) and by immunodetection using a Strep-Tactin-HRP conjugate (lower panel). Results are shown for whole cell lysates of *C. glutamicum* carrying either pPREx2 or pPREx-IolG-Strep and for purified IolG-Strep after affinity chromatography. M, marker proteins with molecular masses indicated in kDa; -, non-induced; +, induced with 1 mM IPTG and p, purified IolG-Strep (~0.5 µg).

4. Conclusions

In the present work, we have demonstrated that the promoter leakiness commonly observed with pEKEx2-based plasmids is due to reduced functionality of the plasmid-encoded repressor LacI, which carries an altered C-terminus, and that duplicate DNA sequences in the pEKEx2 backbone contribute to plasmid instability. Based on this knowledge we constructed the improved pEKEx2-derived expression vectors pPBEx2 and pPREx2, which share the *E. coli/C. glutamicum* shuttle function of their parent, whilst exhibiting restored repressor functionality and lacking the unfavorable replicate DNA sequences. Unlike pEKEx2, pPBEx2/pPREx2 exhibit tight target gene repression in the absence of the inducer IPTG, allowing stringent IPTG-dependent control of expression of the target gene, which is particularly beneficial when production of the recombinant protein, even at low level, is harmful or toxic to the expression host. Moreover, pPREx2 enables production of target proteins carrying a C-terminal Strep-tag II, which facilitates easy protein detection and purification. Thus, for high-level and tightly regulated plasmid-based recombinant protein production in *C. glutamicum*, pPBEx2 and pPREx2 are attractive alternatives to established vectors such as pEKEx2, pAN6, and pCLTON1. Regarding plasmid compatibility, it has been described that pBL1-based vectors are able to co-exist with corynebacterial plasmids such as pCC1, pHM1519 (pCG1) or pGA1 (or derivatives hereof), indicating compatible replicons (Deb and Nath, 1999; Venkova-Canova et al., 2004). According to the general rules of plasmid compatibility (plasmids should carry different replicons and different selection markers), pPBEx2 and pPREx2 (pBL1/kanamycin resistance) are compatible with for instance pVWEx2 (pHM1519/tetracycline resistance) (Wendisch, 1997), pECM3 (pHM1519/chloramphenicol resistance) (Wehmeier et al., 2001), pEC-XT99A (pGA1/tetracycline resistance) (Kirchner and Tauch, 2003), or the recently developed pRG_Duet1 (pCG1/chloramphenicol resistance) (Gauttam et al., 2019). The expression vectors pPBEx2/pPREx2 thus further extend the *C. glutamicum* molecular toolbox for tightly regulated co-expression of multiple genes using controllable promoters.

Author contributions

Patrick J. Bakkes: Conceptualization, Investigation**,** Visualization, Writing – Original Draft, Writing – Review & Editing; **Paul Ramp:** Investigation**,** Visualization, Writing – Original Draft; **Astrid Bida:** Investigation; **Doris Dohmen-Olma:** Investigation; **Michael Bott:** Conceptualization, Writing – Review & Editing; **Roland Freudl:** Conceptualization, Writing – Review & Editing.

Declarations of interest

None.

Funding

This project was financially supported by the CLIB-Competence Center Biotechnology (CKB) funded by the European Regional Development Fund ERDF [grant number 34.EFRE-0300097] and by the German Federal Ministry of Education and Research (BMBF) [grant number 031B0918A], as part of the project “BioökonomieREVIER”.

References

Amann, E., et al., 1988. Tightly regulated *tac* promoter vectors useful for the expression of unfused and fused proteins in *Escherichia coli*. Gene. 69**,** 301-15. doi:10.1016/0378-1119(88)90440-4

Baumgart, M., et al., 2013. Construction of a prophage-free variant of *Corynebacterium glutamicum* ATCC 13032 for use as a platform strain for basic research and industrial biotechnology. Appl Environ Microbiol. 79**,** 6006-15. doi:10.1128/AEM.01634-13

Berman, T., Magasanik, B., 1966. The pathway of myo-inositol degradation in *Aerobacter aerogenes*. Dehydrogenation and dehydration. J Biol Chem. 241**,** 800-6.

Bertani, G., 1951. Studies on lysogenesis. I. The mode of phage liberation by lysogenic *Escherichia coli*. J Bacteriol. 62**,** 293-300.

Brockmeier, U., et al., 2006. Systematic screening of all signal peptides from *Bacillus subtilis*: a powerful strategy in optimizing heterologous protein secretion in Gram-positive bacteria. J Mol Biol. 362**,** 393-402. doi:10.1016/j.jmb.2006.07.034

Bzymek, M., Lovett, S. T., 2001. Instability of repetitive DNA sequences: the role of replication in multiple mechanisms. Proc Natl Acad Sci U S A. 98**,** 8319-25. doi:10.1073/pnas.111008398

Caspers, M., et al., 2010. Improvement of Sec-dependent secretion of a heterologous model protein in *Bacillus subtilis* by saturation mutagenesis of the N-domain of the AmyE signal peptide. Appl Microbiol Biotechnol. 86**,** 1877-85. doi:10.1007/s00253-009-2405-x

Chakerian, A. E., et al., 1991. Evidence for leucine zipper motif in lactose repressor protein. J Biol Chem. 266**,** 1371-4.

Chen, J., Matthews, K. S., 1992. Deletion of lactose repressor carboxyl-terminal domain affects tetramer formation. J Biol Chem. 267**,** 13843-50.

Cohen, S. N., et al., 1972. Nonchromosomal antibiotic resistance in bacteria: genetic transformation of *Escherichia coli* by R-factor DNA. Proc Natl Acad Sci U S A. 69**,** 2110-4. doi:10.1073/pnas.69.8.2110

Crameri, A., et al., 1996. Improved green fluorescent protein by molecular evolution using DNA shuffling. Nat Biotechnol. 14**,** 315-9. doi:10.1038/nbt0396-315

de Boer, H. A., et al., 1983. The *tac* promoter: a functional hybrid derived from the *trp* and *lac* promoters. Proc Natl Acad Sci U S A. 80**,** 21-5. doi:10.1073/pnas.80.1.21

Deb, J. K., Nath, N., 1999. Plasmids of corynebacteria. FEMS Microbiol Lett. 175**,** 11-20. doi:10.1111/j.1574-6968.1999.tb13596.x

Eggeling, L., Bott, M., 2005. Handbook of *Corynebacterium glutamicum*. CRC Press, Boca Raton.

Eggeling, L., Reyes, O., 2005. Handbook of *Corynebacterium glutamicum*: Chapter 23.6 - Plasmid vectors for *Corynebacterium glutamicum*. CRC Press.

Eikmanns, B. J., et al., 1991. A family of *Corynebacterium glutamicum*/*Escherichia coli* shuttle vectors for cloning, controlled gene expression, and promoter probing. Gene. 102**,** 93-8. doi:10.1016/0378-1119(91)90545-m

Eikmanns, B. J., et al., 1994. Nucleotide sequence, expression and transcriptional analysis of the *Corynebacterium glutamicum gltA* gene encoding citrate synthase. Microbiology. 140 (Pt 8)**,** 1817-28. doi:10.1099/13500872-140-8-1817

Freudl, R., 2017. Beyond amino acids: Use of the *Corynebacterium glutamicum* cell factory for the secretion of heterologous proteins. J Biotechnol. 258:101-109. doi:10.1016/j.jbiotec.2017.02.023

Frunzke, J., et al., 2008. Co-ordinated regulation of gluconate catabolism and glucose uptake in *Corynebacterium glutamicum* by two functionally equivalent transcriptional regulators, GntR1 and GntR2. Mol Microbiol. 67**,** 305-22. doi:10.1111/j.1365-2958.2007.06020.x

Gauttam, R., et al., 2019. A step forward: Compatible and dual-inducible expression vectors for gene co-expression in *Corynebacterium glutamicum*. Plasmid. 101**,** 20-27. doi:10.1016/j.plasmid.2018.12.004

Gibson, D. G., 2011. Enzymatic assembly of overlapping DNA fragments. Methods Enzymol. 498**,** 349-61. doi:10.1016/B978-0-12-385120-8.00015-2

743 Goldbeck, O., Seibold, G. M., 2018. Construction of pOGOduet - An inducible, bicistronic vector for
744 synthesis of recombinant proteins in *Corynebacterium glutamicum*. Plasmid. 95**,** 11-15.
745 doi:10.1016/j.plasmid.2018.01.001
746 Green, M. R., Sambrook, J., 2012. Molecular Cloning 4th ed. Cold Spring Harbor Laboratory Press, U.S.
747 Hemmerich, J., et al., 2019. Combinatorial impact of Sec signal peptides from *Bacillus subtilis* and
748 bioprocess conditions on heterologous cutinase secretion by *Corynebacterium glutamicum*.
749 Biotechnol Bioeng. 116**,** 644-655. doi:10.1002/bit.26873
750 Jurischka, S., et al., 2020. A secretion biosensor for monitoring Sec-dependent protein export in
751 *Corynebacterium glutamicum*. Microb Cell Fact. 19**,** 11. doi:10.1186/s12934-019-1273-z
752 Kang, M. K., et al., 2014. Synthetic biology platform of CoryneBrick vectors for gene expression in
753 *Corynebacterium glutamicum* and its application to xylose utilization. Appl Microbiol
754 Biotechnol. 98**,** 5991-6002. doi:10.1007/s00253-014-5714-7
755 Keilhauer, C., et al., 1993. Isoleucine synthesis in *Corynebacterium glutamicum*: molecular analysis of
756 the *ilvB-ilvN-ilvC* operon. J Bacteriol. 175**,** 5595-603. doi:10.1128/jb.175.17.5595-5603.1993
757 Kinoshita, S., et al., 1957. Studies on the amino acid fermentation - Part I. production of L-glutamic acid
758 by various microorganisms. J Gen Appl Mirobiol. 3**,** 193-205.
759 Kirchner, O., Tauch, A., 2003. Tools for genetic engineering in the amino acid-producing bacterium
760 *Corynebacterium glutamicum*. J Biotechnol. 104**,** 287-99. doi:10.1016/s0168-1656(03)00148-
761 2
762 Klaffl, S., et al., 2013. Complex regulation of the phosphoenolpyruvate carboxykinase gene *pck* and
763 characterization of its GntR-type regulator IolR as a repressor of myo-inositol utilization genes
764 in *Corynebacterium glutamicum*. J Bacteriol. 195**,** 4283-96. doi:10.1128/JB.00265-13
765 Kortmann, M., et al., 2015. A chromosomally encoded T7 RNA polymerase-dependent gene expression
766 system for *Corynebacterium glutamicum*: construction and comparative evaluation at the
767 single-cell level. Microb Biotechnol. 8**,** 253-65. doi:10.1111/1751-7915.12236
768 Kraxner, K. J., et al., 2019. The conserved actinobacterial transcriptional regulator FtsR controls
769 expression of *ftsZ* and further target genes and influences growth and cell division in
770 *Corynebacterium glutamicum*. BMC Microbiol. 19**,** 179. doi:10.1186/s12866-019-1553-0
771 Krings, E., et al., 2006. Characterization of myo-inositol utilization by *Corynebacterium glutamicum*:
772 the stimulon, identification of transporters, and influence on L-lysine formation. J Bacteriol.
773 188**,** 8054-61. doi:10.1128/JB.00935-06
774 Laemmli, U. K., 1970. Cleavage of structural proteins during the assembly of the head of bacteriophage
775 T4. Nature. 227**,** 680-5. doi:10.1038/227680a0
776 Lausberg, F., et al., 2012. A tetracycline inducible expression vector for *Corynebacterium glutamicum*
777 allowing tightly regulable gene expression. Plasmid. 68**,** 142-147.
778 doi:10.1016/j.plasmid.2012.05.001
779 Lee, J. Y., et al., 2016. The Actinobacterium *Corynebacterium glutamicum*, an Industrial Workhorse. J
780 Microbiol Biotechnol. 26**,** 807-22. doi:10.4014/jmb.1601.01053
781 Lee, M. J., Kim, P., 2018. Recombinant Protein Expression System in *Corynebacterium glutamicum* and
782 Its Application. Front Microbiol. 9**,** 2523. doi:10.3389/fmicb.2018.02523
783 Menkel, E., et al., 1989. Influence of increased aspartate availability on lysine formation by a
784 recombinant strain of *Corynebacterium glutamicum* and utilization of fumarate. Appl Environ
785 Microbiol. 55**,** 684-8.
786 Parker, S. K., et al., 2007. Purification and characterization of mycobacterial phospholipase A: an
787 activity associated with mycobacterial cutinase. J Bacteriol. 189**,** 4153-60.
788 doi:10.1128/JB.01909-06
789 Pfeifer-Sancar, K., et al., 2013. Comprehensive analysis of the *Corynebacterium glutamicum*
790 transcriptome using an improved RNAseq technique. BMC Genomics. 14**,** 888.
791 doi:10.1186/1471-2164-14-888
792 Ramaley, R., et al., 1979. Purification and properties of *Bacillus subtilis* inositol dehydrogenase. J Biol
793 Chem. 254**,** 7684-90.

794 Ramnath, L., et al., 2017. Identification of lipolytic enzymes isolated from bacteria indigenous to
795 Eucalyptus wood species for application in the pulping industry. Biotechnol Rep (Amst). 15**,**
796 114-124. doi:10.1016/j.btre.2017.07.004
797 Stansen, C., et al., 2005. Characterization of a *Corynebacterium glutamicum* lactate utilization operon
798 induced during temperature-triggered glutamate production. Appl Environ Microbiol. 71**,**
799 5920-8. doi:10.1128/AEM.71.10.5920-5928.2005
800 Stenberg, K. A., Vihinen, M., 2009. Crystal structure of a 1.6-hexanediol bound tetrameric form of
801 *Escherichia coli* Lac-repressor refined to 2.1 Å resolution. Proteins. 75**,** 748-59.
802 doi:10.1002/prot.22284
803 Su, L., et al., 2013. Extracellular location of *Thermobifida fusca* cutinase expressed in *Escherichia coli*
804 BL21(DE3) without mediation of a signal peptide. Appl Environ Microbiol. 79**,** 4192-8.
805 doi:10.1128/AEM.00239-13
806 Venkova-Canova, T., et al., 2004. Characterization of the cryptic plasmid pCC1 from *Corynebacterium*
807 *callunae* and its use for vector construction. Plasmid. 51**,** 54-60.
808 doi:10.1016/j.plasmid.2003.09.002
809 Wehmeier, L., et al., 2001. A *Corynebacterium glutamicum* mutant with a defined deletion within the
810 *rplK* gene is impaired in (p)ppGpp accumulation upon amino acid starvation. Microbiology.
811 147**,** 691-700. doi:10.1099/00221287-147-3-691
812 Wendisch, V. F., 1997. PhD thesis - Heinrich Heine University Düsseldorf.

813